A Correlation for the Diameter of Electrospun Polymer Nanofibers

Matthew E. Helgeson and Norman J. Wagner
Center for Molecular Engineering and Thermodynamics, Dept. of Chemical Engineering, Univ. of Delaware, 150 Academy Street, Newark, DE 19713

DOI 10.1002/aic.11056
Published online November 28, 2006 in Wiley InterScience (www.interscience.wiley.com).

A rational method to control morphology of polymer nanofibers produced by electrospinning is developed using dimensional analysis of the electrospinning process. The analysis is validated against data sets from the literature, which provides an empirical correlation between fiber size, controllable operating conditions, and measurable spinning solution properties. A stable jet operating regime is identified for which scaling of dimensionless groups is presented. Deviations from this scaling are qualitatively consistent with capillary instability of the electrospinning jet, for which a beaded fiber morphology is obtained. The results provide criteria for designing and controlling electrospinning of polymer solutions and resulting nanofiber morphology. © 2006 American Institute of Chemical Engineers *AIChE J,* 53: 51–55, 2007
Keywords: electrospinning, nanofibers, polymer, electrohydrodynamics

Introduction

The rapid development of applications for nanofiber technology in biomaterials,[1–5] electronic and magnetic materials,[6,7] composites,[8] catalysis,[9,10] and sensors[11] motivates the need for a simple, inexpensive process to produce nanofibers, either as non-woven mats or as single elements. Polymer electrospinning has gained much attention recently as a process to produce polymer and composite nanofibers,[12] requiring less time and resources than alternative techniques such as nanotemplating and molecular self-assembly.[8]

The electrospinning process is illustrated in Figure 1. An electrical potential on the order of kilovolts is applied between a capillary, containing a polymer solution or melt, and a grounded collection target. Free charge accumulates on the liquid-air interface of the capillary, which experiences an electrostatic stress due to the applied field, whose strength is determined by the applied potential and the separation distance between the capillary and the target. This electrostatic stress overcomes surface tension and deforms the free surface into a critically stable shape, known as a "Taylor cone."[13,14] Beyond a critical field strength, the free surface becomes unstable, and a jet of fluid is ejected. The jet is elongated by the electric stress, and solvent evaporation results in the formation of polymer fibers that are deposited onto a grounded target.

Despite the widespread and rapidly growing use of electrospinning as a synthesis technique for novel nanomaterials, there are no simple methods of predicting a priori the properties of electrospun fibers *from knowledge of the spinning solution properties and electrospinning operating conditions alone*. The electrospinning of new materials typically follows an ad hoc method of varying fluid concentrations and controlled variables. Thus, a simple analysis leading to estimation of fiber properties (for example, diameter) for novel systems would be highly beneficial in allowing for rapid development of novel nanomaterials.

Several analytical models for electrospinning based on slender body electrohydrodynamic theory[15] have been previously proposed that attempt to predict jet behavior. Stability analysis of electrostatically driven jets by Hohman et al.[16,17] led to the development of operating maps over which different operating regimes could be predicted (such as whipping instability, varicose instability, and stable jetting). More detailed analyses have been presented[18–20] to predict the ultimate diameter of

Correspondence concerning this article should be addressed to N. J. Wagner at wagner@che.udel.edu.

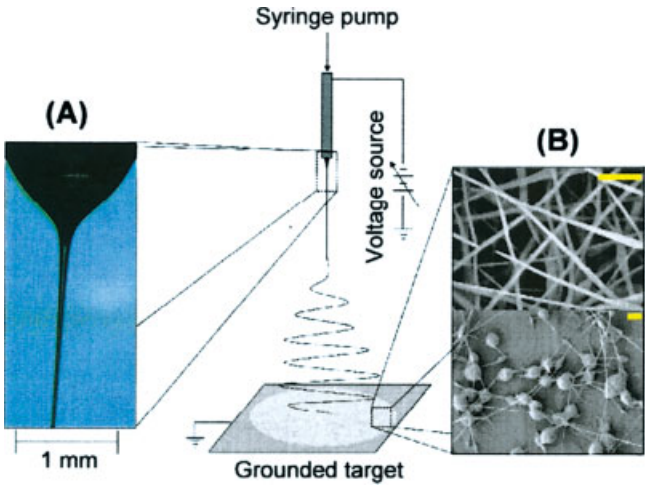

Figure 1. Electrospinning process.

Inset (A) shows a high-speed photograph of a jet of poly(ethylene oxide). Inset (B) shows FESEM micrographs of electrospun poly(ethylene oxide) depicting uniform nanofibers (top) and beaded nanofibers (bottom). The scale bars shown correspond to 1 μm. [Color figure can be viewed in the online issue, which is available at www.interscience.wiley.com.]

electrospinning jets. However, these models all involve internal parameters that are impossible to know a priori and are very difficult to measure in practice. For example, Spivak et al.[20] and Feng[18] developed models to predict the asymptotic behavior of the jet radius in terms of an initial jet radius, which is not known. Similarly, Fridrikh et al.[19] proposed a force balance model for the final diameter of electrospun fibers, but it implicitly contains a "radius of whipping," which has proven difficult to measure or predict, and introduces further approximations for mass transfer to ultimately compare with experimental data. As a result, these models and analyses do not allow for a priori prediction of electrospun nanofiber morphology. However, they do provide a theoretical foundation for the development of a simple scaling analysis relating fiber morphology to spinning solution properties and controllable process parameters.

Several empirical relationships have been proposed for the prediction of electrospun fiber morphology from one fluid property. For example, McKee et al. showed[4,21] that the diameter of electrospun polymer fibers displays a uniform power law scaling with the zero-shear viscosity, η_0, and Shenoy et al.[22] identified the important need to be above the critical entanglement concentration of the polymer to form uniform fibers. However, later results by McKee et al.[23] and Daga et al.[12] show that this result is not universal, especially for fibers spun from hydrogen-bonding systems as well as aqueous polyethylene oxide (PEO). Indeed, when comparing fiber diameter versus η_0 for various neat polymer-solvent systems at different operating conditions, as shown in Figure 2, a large variation in behavior is observed.

Dimensional Analysis

Feng[18] identified the following dimensionless groups as governing parameters for electrospinning in a model developed from conservation equations for mass, momentum, and electrical charge applied to an electrospinning jet of a Newtonian fluid:

$$\mathrm{Pe} = \frac{2\bar{\varepsilon}v_0}{KR_0}, \mathrm{Re} = \frac{\rho v_0 R_0}{\eta_0}, We = \frac{\rho v_0^2 R_0}{\gamma}, \Psi = \frac{\bar{\varepsilon}E_0^2}{\rho v_0^2} \quad (1)$$

The Peclet number, Pe, is a ratio of electrical conduction to convective time scales, representing the motion of free charges relative to the jet motion. The jet Reynolds number, Re, is a ratio of inertial to viscous stresses, representing the kinetic energy of the jet relative to viscous dissipation. The Weber number, We, is a ratio of inertial to surface stresses. Finally, the dimensionless field strength, Ψ, is a ratio of electrostatic to inertial stresses. These dimensionless groups are functions of the dielectric permittivity of atmosphere ($\bar{\varepsilon}$); conductivity (K), density (ρ), zero-shear viscosity (η_0), and surface tension (γ) of the electrospinning fluid; the applied electric field (E_0); and characteristic jet radius (R_0) and velocity (v_0) scales. The characteristic electric field strength E_0 is taken here to be the average field defined as the voltage applied to the capillary tip divided by the working distance between the capillary tip and collecting target, Φ_0/L[24].

These dimensionless groups contain internal variables that cannot be directly controlled or readily measured, namely, R_0 and v_0. It is standard engineering practice to eliminate these internal variables in order to develop useful correlations between dimensionless groups that contain only *measurable* spinning fluid properties and *measurable* electrospinning parameters:

$$\Pi_1 = \mathrm{Re}\ \mathrm{Pe}\ \Psi = \frac{2\bar{\varepsilon}^2\Phi_0^2}{K\eta_0 L^2} \quad (2)$$

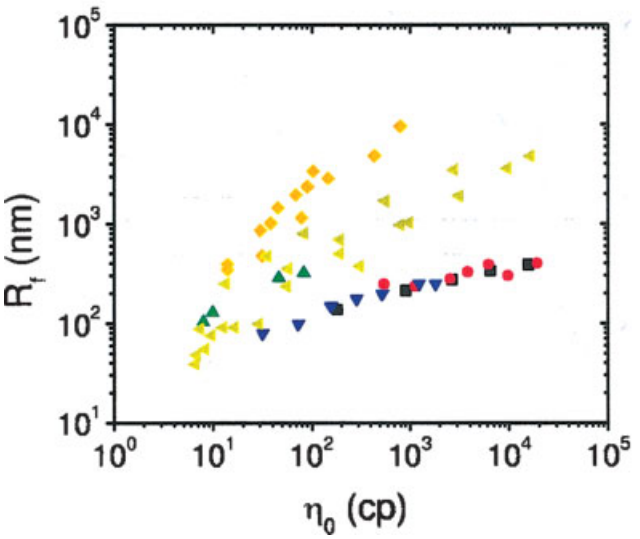

Figure 2. Electrospun fiber diameter versus zero-shear viscosity of solutions of PEO-water[12,28,30] (■, ●, and ▼, respectively), PEO-water-ethanol[29] (△), poly(ethylene terephthalate-*co*-ethylene isophthalate)-chloroform-dimethylformamide[21] (◇), and poly(methyl methacrylate)-dimethylformamide[31] (◀).

[Color figure can be viewed in the online issue, which is available at www.interscience.wiley.com.]

Table 1. Data Used in Dimensional Analysis and Approximate Orders of Magnitude for Parameters

Cited Work	Polymer-Solvent System	η_0 (Pa s)	K (S/m)	γ (N/m)	Φ_0 (V)	L (m)	R_f (m)
Daga et al.[12]	poly(ethylene oxide)-water	10^{-1}–10^{1}	10^{-3}–10^{-2}	75	20,000	0.20	10^{-7}
Deitzel et al.[28]	poly(ethylene oxide)-water	10^{-1}–10^{1}	10^{-3}–10^{-2}	75	7000	0.10	10^{-7}
Drew et al.[29]	poly(ethylene oxide)-ethanol-water	10^{-3}–10^{-1}	10^{-3}–10^{-2}	25	12,000	0.15	10^{-7}
Fong et al.[30]	poly(ethylene oxide)-water	10^{-2}–10^{0}	10^{-3}	75	30,700	0.22	10^{-7}–10^{-6}
McKee et al.[21]	poly(ethylene terepthalate-co-ethylene isophthalate)-chloroform-dimethylformamide	10^{-2}–10^{0}	10^{-3}*	35*	18,000	0.24	10^{-7}–10^{-5}
Gupta et al.[31]	poly(methyl methacrylate)-dimethylformamide	10^{-3}–10^{1}	10^{-3}*	35*	10,000	0.15	10^{-6}–10^{-5}

*Properties were estimated from literature data (see text).

This new dimensionless group, Π_1, is a ratio of the electrostatic ($\bar{\varepsilon}\,\Phi_0^2/L^2$) and electroviscous ($\eta K/\bar{\varepsilon}$) stresses experienced by an electrostatically driven fluid jet, and can be interpreted as a dimensionless stress driving jet elongation. Further, Π_1 contains no internal variables but rather only measurable properties and standard, controllable process parameters.

A second dimensionless group arises by considering a dimensionless electrospun fiber radius R_{jet}/R_0. Elimination of the initial jet radius using the dimensionless groups above yields the following dimensionless electrospun fiber diameter:

$$\Pi_2 = \mathrm{Re}^2\,\mathrm{We}^{-1} = \frac{\rho\gamma R_{jet}}{\eta_0^2} = \mathrm{Oh}^{-2} \tag{3}$$

where we recognize Π_2 as Oh^{-2}, where $\mathrm{Oh} = \frac{\eta_0}{(\rho\gamma R_{jet})^{1/2}}$ is the Ohnesorge number. The Ohnesorge number is known to capture the behavior of free surface flows in which small disturbances lead to capillary breakup of a jet of fluid.[25–27] When Oh $<$ O(1), viscous forces within the jet are insufficient to stabilize disturbances, leading to capillary breakup. As Oh increases above O(1), viscous forces stabilize disturbances at the jet surface, leading to a beads-on-string configuration at intermediate Oh, and stable jets at sufficiently high Oh. Thus, since we have taken R to be the electrospun fiber radius, Oh can be thought of as a characteristic surface stress to express the stability and morphology of electrospinning jets.

In the definition of Oh, the characteristic radius is taken to be the wet radius of the electrospinning jet, R_{jet}. R_{jet} can be computed easily from the dry fiber diameter, R_f, measured, for example, from an electron micrograph such as is shown in Figure 1, by mass balance:

$$R_{jet} = R_f\sqrt{\frac{1}{w_s}} \tag{4}$$

where w_s is the mass fraction of the polymer in the electrospinning fluid. This relationship will be used in the calculation of Oh from measurements of R_f.

It should be noted that the dimensional analysis here does not contain an important operating parameter, the flow rate of fluid supplied to the syringe tip during electrospinning. It is known that adjustment of the flow rate can result in instability of the electrospinning jet.[16,17] However, if the flow rate of material supplied to the syringe tip balances the draw rate of the fluid due to the electric field, and no additional pressure drop is used to drive the flow, the flow rate becomes a dependent variable for the process, and can always be cast in terms of other adjustable parameters (namely, Φ_0 and L). The analysis proposed here presupposes such a definition for steady state operation of the jet.

Results and Discussion

Several data sets presented in the literature[12,21,28–31] and compiled in Table 1 were reduced using the above analysis. The data represent a wide cross-section of the parameter space, including viscosity, surface tension, conductivity, and electric field for several different polymer-solvent systems. Where parameter values were not reported (McKee et al.,[21] and Gupta et al.[31]), the spinning solution surface tension was assumed to be constant and that of the solvent, and conductivity was linearly extrapolated from data for the same or a similar system reported in the literature.[32] For the PEO-water and PEO-water-ethanol systems,[12,28,29] solution conductivity and surface tension were linearly interpolated from data for the same system presented by Fong et al.[30] Operating conditions for the PEO-water-ethanol system[12,28,29] were provided by the investigators.[33] A master plot of Π_1 and Oh (Figure 3) shows a reduction of the data for different systems onto a single master curve

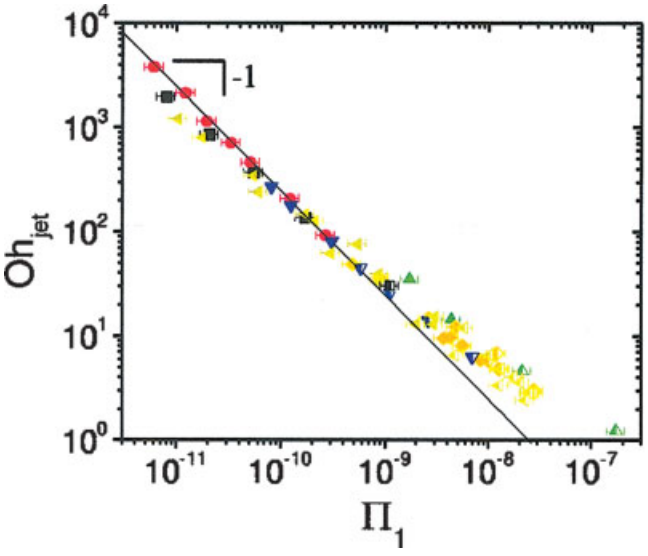

Figure 3. Results of dimensional analysis of electrospinning for several polymer-solvent systems: of PEO-water[12,28,30] (■, ●, and ▼, respectively), PEO-water-ethanol[29] (△), poly(ethylene terephthalate-*co*-ethylene isophthalate)-chloroform-dimethylformamide[21] (◇), and poly(methyl methacrylate)-dimethylformamide[31] (◀).

Error bars represent confidence in estimated solution properties. [Color figure can be viewed in the online issue, which is available at www.interscience.wiley.com.]

(note that Figures 2 and 3 are plotted on the same scale). This suggests that the dimensionless electrostatic stress, Π_1, and the dimensionless surface stress, Oh, are fundamental to understanding polymer solution electrospinning and are strongly correlated with each other. Figure 3, thus, provides a method to calculate, a priori, the approximate fiber size resulting from a stable, electrospinning operation on a neat polymer solution.

Examining Figure 3 more critically shows that beaded fibers (half-filled symbols in Figure 3) first appear below a critical value of Oh specific to each individual polymer-solvent system. This can be predicted in terms of capillary breakup of the electrospinning jet.[26] A decreasing in Oh implies that viscous forces become insufficient to stabilize capillary waves that grow and the jet becomes unstable in this regard, resulting in a beaded morphology or, ultimately, electrospraying at sufficiently low Oh. Shenoy et al.[22] argue that polymer solutions must be above a critical polymer entanglement density to avoid beading, which suggests viscoelasticity may also play a role in dampening surface disturbances. Consequently, the experimental results considered here show that the critical Oh number is not unique across different spinning solutions, such that Oh alone is insufficient to predict the onset of beading, and additional material properties must be important in determining jet stability. The obvious candidate is elongational viscosity, which is not trivially related to the shear viscosity for entangled polymer solutions, and is well known to affect jet stability.[34]

Empirical trends in the master plot are evident in two regimes. First, at large Oh, an inverse linear relationship is evident, such that $\mathrm{Oh} \propto \Pi_1^{-1}$ (solid line, Figure 3). Thus, for large Oh,

$$\Pi_1 \mathrm{Oh} = \frac{2\varepsilon^2 \Phi_0^2}{KL^2(\rho\gamma R_{jet})^{1/2}} = 2.5 \pm 0.2 \times 10^{-8} \qquad (5)$$

Note that this product is *independent of the solution zero-shear viscosity*, suggesting that, in the stable jet limit, correlation with solution zero-shear viscosity is, as noted above, insufficient to accurately describe the final diameter of electrospun fibers across variations in processing and solution conditions and compositions. Rather, the empirical relationship in Eq. 5 provides an estimate for the diameter of electrospun polymer fibers directly in terms of the spinning solution conductivity, surface tension, and operating parameters. Note that the model predictions by Fridrikh et al.,[19] in which the fiber diameter depends only on the balance of electrostatic and surface forces of the jet, also does not explicitly contain the spinning fluid's shear viscosity. Thus, it can be presumed that, in the stable jet operating regime, the fiber morphology is dominated by the equilibrium of these forces as captured by Eq. 5. However, no direct comparison can be made between the correlation developed in this work and the model by Fridrikh et al., as the latter contains internal parameters that cannot be readily measured.

At small values of Oh (less than 100), the data deviate from the inverse scaling, and approach something closer to a $-3/4$ slope. This deviation from the stable jet scaling can be anticipated from consideration of capillary instability of the electrospinning jet, even though the observed power law behavior is merely empirical. Capillary instability manifests as beading along the jet filament, which decreases the radius of the fiber between beads.[34] It is this fiber diameter that is used in the analysis, and it appears in the dominator of the ordinate. Thus, the decrease in fiber radius due to beading causes the positive deviation from the stable jet scaling in this simple manner.

Conclusions

In summary, elimination of internal variables in a dimensional analysis of the electrospinning of a Newtonian fluid provides a robust correlation between the dimensionless fiber radius, as characterized by the Ohnesorge number, and a new dimensionless group Π_1 relating controllable operating parameters and measurable solution spinning properties. A stable jet operating regime has been defined above a critical value of $\mathrm{Oh} \sim \mathrm{O}(100)$, where the simple relationship given in Eq. 5 can be used to predict the electrospun fiber diameter. Below $\mathrm{Oh} \sim \mathrm{O}(100)$, a transition to a weaker dependence on the dimensionless electrostatic stress is obtained and beading becomes evident.

The applicability of these results to more complex systems, such as polymer-nanoparticle composites, is questionable[12] because of the nonlinear extensional rheology typical of such electrospinning solutions. Extensions of this analysis to fluids with strong extensional thickening, for example, will require considerations of the non-Newtonian fluid properties and their influence both on jet formation and jet stability.

Acknowledgments

The authors gratefully thank Dr. Christopher Drew for correspondence, as well as Dr. Joseph Deitzel for use of the high-speed photography equipment and helpful conversations. The original authors of literature data compiled in this work are also duly acknowledged. Electron microscopy was performed at the Keck Electron Microscopy Facility with the assistance of Dr. Chaoyang Ni and Frank Kriss. Funding for this work was partly provided by the National Science Foundation (DMR-0210223).

Literature Cited

1. Brewster ME, Verreck G, Chun I, Rosenblatt J, Mensch J, Van Duck A, Noppe M, Arien A, Bruining M, Peeters J. The use of polymer-based electrospun nanofibers containing amorphous drug dispersions for the delivery of poorly water-soluble pharmaceuticals. *Pharmazie*. 2004;59(5):387–391.
2. Jia HF, Zhu GY, Vugrinovich B, Kataphinan W, Reneker DH, Wang P. Enzyme-carrying polymeric nanofibers prepared via electrospinning for use as unique biocatalysts. *Biotechnol Prog*. 2002;18(5):1027–1032.
3. Lim TC, Kotaki M, Yang TKJ, Fujihara K, Ramakrishna S. Recent advances in tissue engineering applications of electrospun nanofibers. *Materials Technol*. 2004;19(1):20–27.
4. McKee MG, Layman JM, Cashion MP, Long TE. Phospholipid nonwoven electrospun membranes. *Science*. 2006;311(5759):353–355.
5. Casper CL, Stephens JS, Tassi NG, Chase DB, Rabolt JF. Controlling surface morphology of electrospun polystyrene fibers: effect of humidity and molecular weight in the electrospinning process. *Macromol*. 2004;37(2):573–578.
6. Choi SW, Jo SM, Lee WS, Kim YR. An electrospun poly(vinylidene fluoride) nanofibrous membrane and its battery applications. *Adv Materials*. 2003;15(23):2027–2032.
7. Drew C, Wang XY, Senecal K, Schreuder-Gibson H, He JN, Kumar J, Samuelson LA. Electrospun photovoltaic cells. *J Macromol Sci—Pure Appl Chem*. 2002;A39(10):1085–1094.
8. Huang ZM, Zhang YZ, Kotaki M, Ramakrishna S. A review on polymer nanofibers by electrospinning and their applications in nanocomposites. *Compos Science Technol*. 2003;63(15):2223–2253.
9. Caruso RA, Schattka JH, Greiner A. Titanium dioxide tubes from sol-gel coating of electrospun polymer fibers. *Adv Materials*. 2001; 13(20):1577–1579.

10. Dong H, Jones WE. New catalyst supports for palladium nanoparticles: carbonized and metal oxide nanofibers prepared by electrospinning. *Abstracts Papers of Am Chem Soc*. 2004;228:U826–U827.
11. Patel AC, Li SX, Yuan JM, Wei Y. In situ encapsulation of horseradish peroxidase in electrospun porous silica fibers for potential biosensor applications. *Nano Lett*. 2006;6(5):1042–1046.
12. Daga V, Helgeson ME, Wagner NJ. Electrospinning of neat and laponite-filled aqueous poly(ethylene oxide) solutions. *J Polym Sci B—Polym Phys*. 2006;44:1608–1617.
13. Taylor G. Electrically driven jets. *Proc R Soc: London*. 1969;313:453–75.
14. Yarin AL, Koombhongse S, Reneker DH. Taylor cone and jetting from liquid droplets in electrospinning of nanofibers. *J Appl Phys*. 2001;90(9):4836–4846.
15. Saville DA. Electrohydrodynamics: the Taylor-Melcher leaky dielectric model. *Ann Rev Fluid Mech*. 1997;29:27–64.
16. Hohman MM, Shin M, Rutledge G, Brenner MP. Electrospinning and electrically forced jets. I. Stability theory. *Phys Fluids*. 2001;13(8):2201–2220.
17. Hohman MM, Shin M, Rutledge G, Brenner MP. Electrospinning and electrically forced jets. II. Applications. *Phys Fluids*. 2001;13(8):2221–2236.
18. Feng JJ. Stretching of a straight electrically charged viscoelastic jet. *J Non-Newtonian Fluid Mech*. 2003;116(1):55–70.
19. Fridrikh SV, Yu JH, Brenner MP, Rutledge GC. Controlling the fiber diameter during electrospinning. *Phys Rev Lett*. 2003;90(14):144502.
20. Spivak AF, Dzenis YA, Reneker DH. A model of steady state jet in the electrospinning process. *Mech Res Commun*. 2000;27(1):37–42.
21. McKee MG, Wilkes GL, Colby RH, Long TE. Correlations of solution rheology with electrospun fiber formation of linear and branched polyesters. *Macromol*. 2004;37(5):1760–1767.
22. Shenoy SL, Bates WD, Frisch HL, Wnek GE. Role of chain entanglements on fiber formation during electrospinning of polymer solutions: good solvent, non-specific polymer-polymer interaction limit. *Polymer*. 2005;46(10):3372–3384.
23. McKee MG, Elkins CL, Long TE. Influence of self-complementary hydrogen bonding on solution rheology/electrospinning relationships. *Polymer*. 2004;45(26):8705–8715.
24. It should be noted that the electric field is known to vary widely across the coordinate of the jet. However, the quantity used here serves as an appropriate order of magnitude estimate of the electric field experienced by the electrospinning jet.
25. Christanti Y, Walker LM. Effect of fluid relaxation time of dilute polymer solutions on jet breakup due to a forced disturbance. *J Rheol*. 2002;46(3):733–748.
26. Lopez-Herrera JM, Ganan-Calvo AM. A note on charged capillary jet breakup of conducting liquids: experimental validation of a viscous one-dimensional model. *J Fluid Mech*. 2004;501:303–326.
27. Wong DCY, Simmons MJH, Decent SP, Parau EI, King AC. Break-up dynamics and drop size distributions created from spiralling liquid jets. *Int J Multiphase Flow*. 2004;30(5):499–520.
28. Deitzel JM, Kleinmeyer J, Harris D, Tan NCB. The effect of processing variables on the morphology of electrospun nanofibers and textiles. *Polymer*. 2001;42(1):261–272.
29. Drew C, Wang XY, Samuelson LA, Kumar J. The effect of viscosity and filler on electrospun fiber morphology. *J Macromol Sci—Pure Appl Chem*. 2003;A40(12):1415–1422.
30. Fong H, Chun I, Reneker DH. Beaded nanofibers formed during electrospinning. *Polymer*. 1999;40(16):4585–4592.
31. Gupta P, Elkins C, Long TE, Wilkes GL. Electrospinning of linear homopolymers of poly(methyl methacrylate): exploring relationships between fiber formation, viscosity, molecular weight and concentration in a good solvent. *Polymer*. 2005;46(13):4799–4810.
32. Wang A, Hsieh AJ, Rutledge GC. Electrospinning of poly(MMA-co-MAA) copolymers and their layered silicate nanocomposites for improved thermal properties. *Polymer*. 2005;46(10):3407–3418.
33. Drew C. Private Communication.
34. Christanti Y, Walker LM. Surface tension driven jet break up of strain-hardening polymer solutions. *J Non-Newtonian Fluid Mech*. 2001;100(1–3):9–26.

Manuscript received Jun. 19, 2006, and revision received Sept. 15, 2006.